Low frequency dielectric relaxation phenomena in conducting polypyrrole and conducting polypyrrole-zeolite composites

A. N. Papathanassiou[a)]
Section of Solid State Physics, Department of Physics, University of Athens, Panepistimiopolis, GR 157 84 Zografos, Greece and Hellenic Army Academy, GR 166 73 Vari, Greece

J. Grammatikakis and I. Sakellis
Section of Solid State Physics, Department of Physics, University of Athens, Panepistimiopolis, GR 157 84 Zografos, Greece

S. Sakkopoulos and E. Vitoratos
Department of Physics, University of Patras, GR 265 00 Patras, Greece

E. Dalas
Department of Chemistry, University of Patras, GR 265 00 Patras, Greece

(Received 8 January 2004; accepted 9 July 2004)

The dielectric properties of polypyrrole-zeolite composites up to 50% w/w zeolite are studied in the frequency range from 10^{-2} to 2×10^{6} Hz from room temperature to liquid nitrogen temperature. The complex permittivity formalism reveals a temperature dependent relaxation in all samples except for the 25% w/w zeolite composite. The frequency f_{max} where a maximum of a loss peak is located varies with temperature by the Williams-Lander-Ferry law. The values of the activation energy of the relaxation process (which are of the order of polaronic dc conductivity) have the tendency to reach a minimum in the 25% w/w composition, which is a loss-free composite. The 50% w/w zeolite behaves as a dielectric where ionic relaxation dominates. The temperature variation of the strength of the dielectric mechanism follows a Curie law, apart from 50% w/w zeolite where the dielectric strength is practically constant. The frequencies, where loss peaks are maximum, as well as dc conductivity follow qualitatively the same temperature law, but the parameters are quite different. Moreover, the locations of the relaxation peaks diverge from the predictions of Barton-Nakajima-Namikawa model. Long-range electric charge transport (dc conductivity) and the relaxation that corresponds to short-range localized motion probably involve different processes. © *2004 American Institute of Physics*. [DOI: 10.1063/1.1788846]

I. INTRODUCTION

Electric charge transport in conducting polypyrrole is the subject of numerous theoretical and experimental investigations. The objectives are the construction of a generalized frame for electrical conductivity in conducting polymers[1,2] and the preparation of well characterized metallic or semiconducting polymers for many different technological applications, such as solar cells, *p*H electrodes, media for hydrogen storage, and electronic devices.[3–5] Zeolite contains pores, channels, and cages of different dimensions and shapes, and their surface is negatively charge-balanced with exchangeable cations.[4] Polypyrrole may complex with zeolite in composites that are characterized by the fast electronic mobility of polypyrrole and the capability of zeolite to incorporate cations into his structure. The question that arises in such materials, where electronic and ionic conduction coexist, is how the composition of such mixtures affects their effective electric and dielectric behavior. As we will see in this paper, the nature of the composite is metallic (in the absence of loss) at 25% w/w zeolite and dielectric in the 50% w/w zeolite.

[a)]Author to whom correspondence should be addressed; electronic mail: apapathan@in.gr

II. EXPERIMENT

Freshly distilled pyrrole (Merc AR) was polymerized in the presence of $FeCl_3$ as oxidant in hydrochloric acid–water solutions at *p*H=2.00 in an ice bath. The molar ratio of oxidant to monomer was 1:1 and the solvent used was triply distilled water. Polypyrrole was obtained as black powder and was purified by Soxhlet extraction for 36 h.[6] Zeolite was purified according to the following procedure.[7,8] First, it was dispersed in distilled water and the emulsion was stirred for 24 h. The suspension then was purified by sedimentation to collect the <2 μm in diameter fraction, washing with 1*M* CH_3COONa and CH_3COOH (*p*H=5) to remove carbonate. Then washing with 0.3*M* sodium citrate and *1M* $NaHCO_3$ and $Na_2S_2O_4$ to remove free iron sulfide took place. The precipitate was dispersed in 100 ml 1*N* NaCl and was stirred for 30 min. The emulsion was repeatedly centrifuged in order to obtain the same type of exchange cations. Purified zeolite was added to the polypyrrole solutions in the proper quantity to obtain 10%, 25%, 35%, and 50% w/w content of the zeolite. The precipitates were washed with 1*N* HCl and dried overnight under nitrogen atmosphere. From these polypyrrole/zeolite disk shaped specimens 13 mm in diameter and about 1.5 mm thick were made in an IR press.

The samples were placed in the sample holder of a

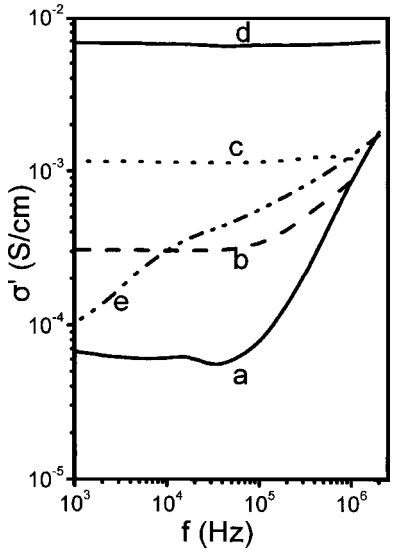

FIG. 1. The real part of the conductivity vs frequency at room temperature ($T=296$ *K*) for conducting polypyrrole and composites. (a) polypyrrole, (b) 10 wt % zeolite, (c) 25 wt % zeolite, (d) 35 wt % zeolite, (e) 50 wt % zeolite.

vacuum cryostat operating at 1 Pa. Good contact between the surfaces of the specimen and the electrodes was achieved by using silver paste. The temperature was monitored from room temperature to liquid nitrogen temperature. The measurements were performed in the frequency range from 10^{-2} to 2×10^{6} Hz by a Solartron SI 1260 impedance analyzer.

III. RESULTS AND DISCUSSION

In amorphous materials, charge carriers usually move along the specimen from one electrode to the other (dc conduction) at low frequencies. The conductivity increases as the charge entities make better use of neighboring sites and move along short-range distance.[9] For hopping transport, the increase of the frequency involves more electronic states, since the transition rate between them is larger than the value of the frequency of the applied field.[10] The imaginary part of the conductivity σ' at room temperature is plotted in Fig. 1 as a function of the frequency f of the external electric field for polypyrrole and polypyrrole-zeolite composites. For polypyrrole and three of the polypyrrole-zeolite composites, in the low frequency region, the conductivity is frequency independent and holds a constant value σ_0. Above the dc plateau, the conductivity increases sublinearly according to the empirical fractional law[10,11]

$$\sigma'(\omega) = \sigma_0 + A\omega^{n}, \tag{1}$$

where ω is the angular frequency ($\omega=2\pi f$, f is the frequency of the applied electric field), σ_0 is the dc conductivity, A is a constant, and $0<n\leqslant 1$. The dc plateau is lacking in the 50% w/w zeolite composite. It is evident that low frequency dispersion[12] (LFD) dominates. This idea seems reasonable: as the composite is significantly rich in zeolite, which is an ionic conductor, ionic relaxation phenomena are prominent (e.g., space-charge polarization and/or bulk LFD). For compositions up to 35% wt zeolite, polypyrrole-zeolite composites behave qualitatively as polypyrrole, i.e., as metallic polymers. At 50% w/w zeolite, the effective response of the blend resembles that of a dielectric.

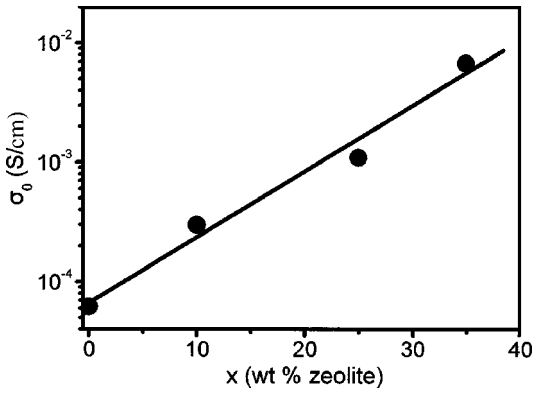

FIG. 2. The frequency-independent real part of the conductivity σ_0 (dc conductivity) measured at room temperature as a function of the % w/w zeolite in polypyrrole-zeolite composites.

In Fig. 2, the room temperature frequency-independent conductivity σ_0 (which, in principle, can be identified as the dc conductivity) is plotted as a function of the weight percentage content x in zeolite. As mentioned in the preceding paragraph, no dc plateau is observed for $x=50\%$. It is worth noticing that the conductivity increases exponentially with the weight percentage in zeolite, at a rate

$$\frac{d\ln\sigma_0}{dx} = (0.055\pm0.005)\ (0\leqslant x\leqslant 35\%). \tag{2}$$

Protonated polypyrrole is the highly conducting phase in comparison with the ionic conductivity of zeolite. As the composites become poor in polypyrrole (increasing x), the effective conductivity of the specimen should decrease, which contradicts our experimental results. The phenomenon may be understood recalling that zeolite is an electroactive material that causes additional (inherent) protonation of polypyrrole that adds to the extrinsic doping procedure with aqueous HCl acid.

In the formalism of the complex permittivity, the transition of the dc plateau to dispersive σ' as frequency increases results in the appearance of a relaxation peak. The real and the imaginary parts of the permittivity are related, respectively, with the real and the imaginary parts of the complex conductivity:

$$\varepsilon'(\omega) = \varepsilon_\infty + \frac{\sigma''(\omega)}{\varepsilon_0\omega}, \tag{3}$$

$$\varepsilon''(\omega) = \frac{\sigma'(\omega)}{\varepsilon_0\omega} = \frac{\sigma_0}{\varepsilon_0\omega} + \varepsilon_d'', \tag{4}$$

where ε_0 is the permittivity of free space, ε_∞ is the high-frequency permittivity, σ_0 is the dc conductivity, and ε_d'' is the imaginary part of the permittivity after subtracting the dc component,

$$\varepsilon_d'' = \frac{\sigma'(\omega)-\sigma_0}{\varepsilon_0\omega}. \tag{5}$$

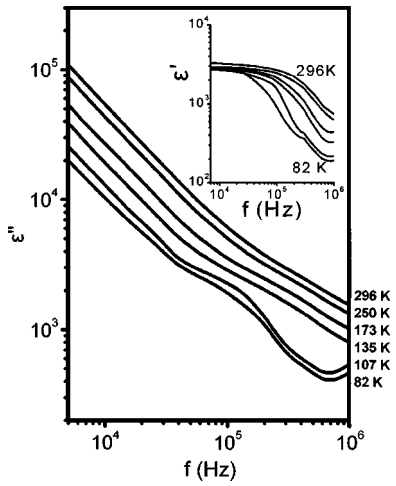

FIG. 3. The imaginary part of the dielectric constant vs frequency at different temperatures for the 10% w/w zeolite 123 composite. The inset shows the real part of the dielectric constant vs frequency.

The real and the imaginary parts of the dielectric constant vs frequency at different temperatures for the 10% w/w zeolite blend are depicted in log-log representation in Fig. 3. At a given temperature, $\log \varepsilon''(\log f)$ decreases linearly in the low-frequency range with slope equal to -1, while a divergence is observed in the high-frequency part. As temperature decreases, ε'' is suppressed due to the reduction of the dc conductivity and a "knee" in the high frequency range becomes more obvious. In Fig. 4, we give a typical log-log representation of the measured imaginary part of the permittivity, a straight line corresponding to the dc contribution and the relaxation peak resulting after subtracting the dc contribution from the measured dataset, following Eq. (5). A similar picture is observed in polypyrrole and the 35% w/w zeolite composite. For the 25% w/w zeolite, no relaxation is traced in the whole frequency range; i.e., the log-log representation of $\varepsilon^{\|}(f)$ is a straight line with slope -1, indicating a constant dc value σ_0 throughout the entire frequency range.

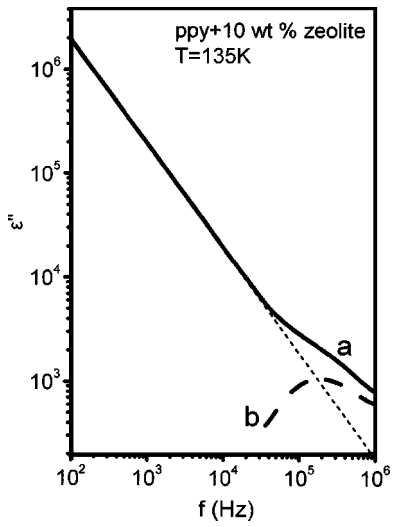

FIG. 4. The measured imaginary part of the permittivity vs frequency at 135 K for 10% w/w zeolite [curve (a)]. The dc component is represented by a straight line with slope equal to -1 (dotted line). The relaxation peak is plotted by dashed curve [curve (b)].

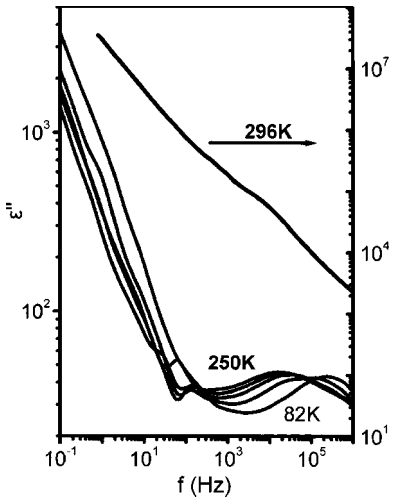

FIG. 5. The imaginary part of the permittivity vs frequency of 50% w/w zeolite for different temperatures. The whole frequency region is dispersive (i.e., frequency-independent values of the conductivity are lacking).

A dc region is lacking in 50% w/w zeolite blend, where the imaginary part of the permittivity decreases sublinearly with frequency (Fig. 5). It is worth noticing that for the composite with 50% w/w zeolite there is a drastic jump in $\varepsilon^{\|}$ from 250 K to 296 K (Fig. 5). This picture is entirely different from that of polypyrrole and the other blends, where a gradual and continuous increase in $\varepsilon^{\|}$ with temperature occurs: the picture presented for the blend with 10% w/w zeolite (Fig. 3) is representative for these specimens. In Fig. 6, where the real part of the permittivity is depicted as a function of frequency, we observe that polarization effects (electrode polarization or LFD) dominate in the low frequencies. It seems that the 50% w/w zeolite composite exhibits an effective dielectric nature and departs from the semiconducting feature of the other specimens. Despite the strong low-frequency polarization phenomena, a relaxation mechanism

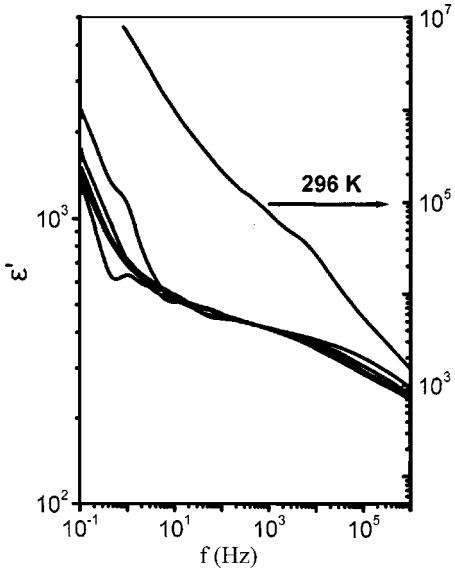

FIG. 6. The real part of the permittivity vs frequency of 50% w/w zeolite for different temperatures. The low-frequency region suffers from low-frequency dispersion (probably electrode effects or low-frequency dispersion LFD).

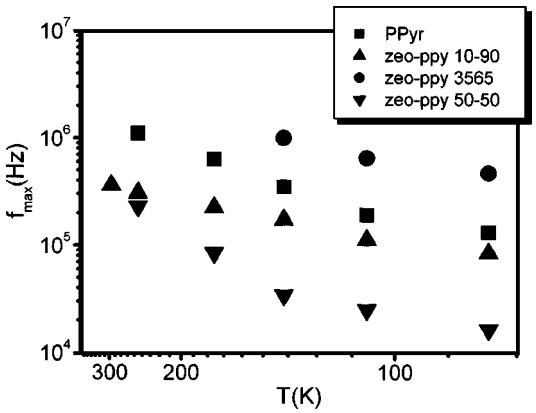

FIG. 7. The frequency f_{max} where a relaxation peak has its maximum vs temperature. Note that no peak is observed in 25% w/w zeolite, while, in 50% w/w zeolite, the maximum was determined directly from Fig. 5.

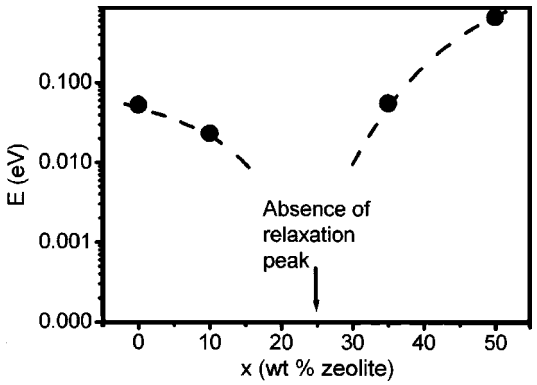

FIG. 8. The activation energy of the relaxation proccess vs the percentage weight concentration in zeolite. The dashed line is drawn to guide the eye.

is well observed in the high-frequency range (Fig. 5). Fortunately enough, it is possible to have a direct (i.e., without subtracting the dc contribution) estimate of the maximum location and the strength of the dielectric response.

The frequency f_{max} where a relaxation peak has its maximum provides the relaxation time τ:

$$\tau(T) = 1/2\pi f_{max}(T). \tag{6}$$

In Fig. 7, f_{max} is presented against temperature. The experimental data follow neither a simple Arrhenius law,

$$f_{max} = f_0 \exp\left(-\frac{E}{kT}\right), \tag{7}$$

nor an Eyring[13] one,

$$f_{max} = f_0 T \exp\left(-\frac{E}{kT}\right), \tag{8}$$

where f_0 is a preexponential constant, E denotes the activation energy, and k is the Boltzmann's constant. We have used a Williams-Lander-Ferry (WLF) relation[14] to match the experimental results:

$$f_{max} = f_0 \exp\left(-\frac{T_1}{T+T_0}\right), \tag{9}$$

where T_1 and T_0 are constants. The activation energy is now $E=kT_1$. The parameters obtained from the fitting of the last equation [Eq. (9)] to the experimental data appearing in Fig. 7 are enlisted in Table I. Note that, for the 35% w/w zeolite we just performed 200 iterations, because only three data points were available and a nonlinear least-squares fit failed to provide a converging solution. Although the WLF model describes *qualitatively* well the experimental results of the sample with 50 wt % zeolite, it yields significant errors in determining the parameters of Eq. (9). Starting from polypyrrole, the activation energy E decreases on increasing content of zeolite, to about 25% w/w zeolite where no relaxation peak is observed. Subsequently, as the composite becomes rich in zeolite ($x \rightarrow 50\%$), the activation energy augments and reaches a value of 0.68 eV, which is reasonable for ionic relaxation rather than polaron hopping relaxation. The activation energies for relaxation in polypyrrole, 10% w/w and 35% w/w composites, are of the order of polaron hopping.[15] For 50% w/w is large enough, the polypyrrole-rich composites relaxation proceeds through polaron hopping; the relaxation in 50% w/w zeolite is determined mainly by ionic motion, obviously, due to the considerable concentration in zeolite. It is apparent that the lack of relaxation in 25% w/w zeolite coincides with the tendency of the activation energy values to reach a minimum (Fig. 8). It seems that, as x tends to 25%, it is more energetically favored for the electric charge carriers to contribute to long-range transfer (dc conductivity) than hopping forward and backward in short-range distance.

The curvature observed in the $f_{max}(T)$ diagrams (Fig. 7) is related with the phenomenological *apparent* activation energy E_{app}, which is defined as the percentage variation of the relaxation time upon T^{-1} [$E_{app} \equiv d \ln \tau(T)/d(1/kT) = -d \ln f_{max}(T)/d(1/kT)$] and increases at high temperatures. This behavior is opposite to that observed in dipolar relaxation, where E_{app} decreases on increasing temperature.[16]

TABLE I. The parameters obtained by fitting the Williams-Lander-Ferry (WLF) model [Eq. (9)] to the frequency values f_{max} where the relaxation peaks reach a maximum. For the 35% w/w zeolite we just performed 200 iterations, because only three data points were available and a nonlinear least-squares fit failed to provide a converging solution.

x (wt % zeolite)	f_0 (Hz)	T_r (K)	T_0 (K)	E (eV)
0 (Ppy)	$(8.03\pm0.09)\times10^6$	617±5	63.3±0.9	0.0532±0.0004
10	$(8.1\pm0.7)\times10^5$	272±4	37±1	0.0234±0.003
25		No relaxation peak appears		
35	$(1.5\pm0.6)\times10^7$	650±80	100±30	0.056±0.006
50	$(5.3\pm0.2)\times10^8$	7900±500	530±20	0.68±0.04

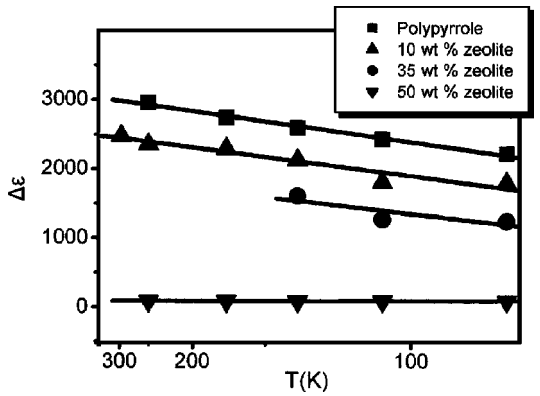

FIG. 9. The dielectric strength $\Delta\varepsilon=\varepsilon_s-\varepsilon_\infty$ of the relaxations vs temperature. The lines are best fits to the data points.Note that the 25% w/w zeolite is free from relaxation, while in 50% w/w zeolite, the strength was estimated directly from the intensity of the relaxations depicted in Fig. 5.

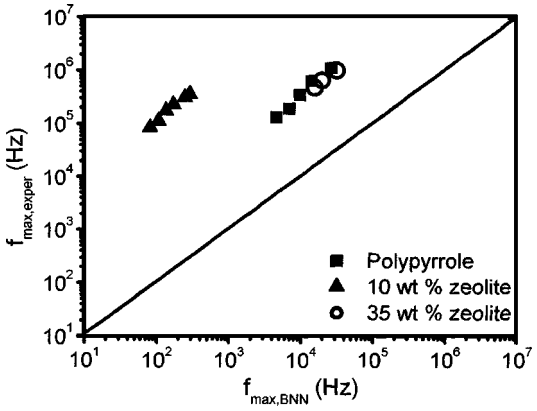

FIG. 10. :The frequency $f_{max,exp}$ where a relaxation peak has its maximum obtained from the experimental results against the frequency $f_{max,BNN}$ predicted by the BNN model. In the absence of a frequency independent conductivity σ_0 for 50% w/w zeolite, no predicted values are available for this sample.

Such behavior has been observed in conducting polymers.[16] In Fig. 9, the intensity of the relaxation peaks $\Delta\varepsilon=\varepsilon_s-\varepsilon_\infty$ is plotted as a function of inverse temperature. It is likely that the relaxation strength varies with temperature according to the Curie law $\Delta\varepsilon\propto T^{-1}$, an aspect predicted by the random free-energy barrier model.[9] The sole exception is the 50% w/w zeolite, where $\Delta\varepsilon$ is practically constant. It is evident that the nature of the relaxation mechanism in the 50% w/w zeolite differs from that observed in the other blends. The intense electrode polarization or LFD, the inefficiency in fitting the WLF model to the $f_{max}(T)$ data, and the insensitivity of the strength $\Delta\varepsilon$ upon temperature indicate that the system behaves as a dielectric, which is dominated by dipolar response.

Barton, Nakajima, and Namikawa (BNN)[17–19] suggested that the position of the relaxation mechanism be determined by the dc conductivity, through the so-called BNN condition:

$$f_{max,BNN}=\frac{1}{2\pi p}\frac{\sigma_0}{\varepsilon_0\Delta\varepsilon}, \tag{10}$$

where p is a constant of the order of unity. Efforts to correlate dielectric relaxation and dc electrical conductivity in conducting polymers have been made in past few years.[16,20,21] In Fig. 10, the experimental values of f_{max} are displayed vs $f_{max,BNN}$. Significant discrepancy occurs between experimental results and theory. The data sets seem as if they were shifted parallel to the predictions (solid line) of the BNN model (Fig. 10). Such disagreement (although to smaller degree) has been observed in some amorphous materials. They were attributed to oversimplifications of the theoretical model: the material characteristics and the nature of charge carriers are ignored, a fixed hopping mechanism is assumed, dipole relaxation and many-body long-range interaction are ignored, etc.[16]

Alternatively, the frequency-independent conductivities σ_0, which result from the dc plateau, vs temperature may be interpreted through the Sheng[22] model, which assumes regions of metallic conductivity separated by insulating barriers. Fluctuation-induced tunneling results in the following temperature variation of the dc conductivity in polypyrrole:[15]

$$\sigma_0(T)=C\exp\left(-\frac{T_1}{T+T_0}\right), \tag{11}$$

where C is constant. The results of fitting Eq. (1) to the experimental $\sigma_0(T)$ are shown in Table II. Of course, in the absence of a dc plateau in the 50% w/w zeolite, no fitting results are enlisted for this specimen. The fitting is poor for the blend with 50% w/w zeolite indicating that the Sheng model can hardly describe the conductivity process in this blend. Both σ_0 and f_0 vary qualitatively the same way with temperature. The negative value of T_1 enlisted in this table is physically unreasonable. According to the Sheng's model $T_0=T_1(2mE)^{-1/2}(\eta/2s)$, where m is the effective mass of the transferring charge, E is the height of the effective potential barrier separating neighboring conducting grains, η is the Planck's constant, and s is the distance between conducting grains.[22] The apparent qualitative agreement stems from the similarity between the formalism of the WLF and Sheng equations. The parameters T_1 and T_0 included in Table I are much different than those of Table II, indicating that relaxation and dc conductivity are two independent processes. As a result, the activation energy of the relaxation process fails to provide information about the conduction process in the present system. The divergence between the fitting parameters of the relaxation and the dc conductivity supports the idea that has risen from the failure of the BNN model to predict the location of the relaxation peaks and states

TABLE II. Parameters of the Sheng's model obtained by fitting Eq. (10) to the $\sigma_0(T)$ data, which are determined from the dc plateau in the conductivity vs frequency representation. Note that in the 50% w/w zeolite composite, the frequency independent region is missing due to low-frequency dispersion. As explained in the text, negative values are physically unreasonable.

x (wt % zeolite)	C (S/cm)	T_1 (K)	T_0 (K)	E (eV)
0 (Ppy)	$(4\pm1)\times10^{-4}$	800±200	100±40	0.07±0.02
10	$(6\pm9)\times10^{-3}$	2000±2000	300±200	0.2±0.2
25	$(6\pm4)\times10^{-3}$	1100±400	220±80	0.09±0.03
35	$(1.8\pm0.7)\times10^{-2}$	200±100	−10±50	0.02±0.01

that dc conductivity and relaxation seem noncorrelated in polypyrrole-zeolite composites.

IV. CONCLUSIONS

The dielectric properties of polypyrrole-zeolite composites up to 50% w/w zeolite are strongly controlled by the concentration of zeolite. The real part of the conductivity vs frequency is characterized by a dc plateau followed by a dispersive high-frequency region in conducting polypyrrole, 10% w/w and 35% w/w zeolite, in polypyrrole-zeolite composites. In the formalism of the complex permittivity, the dispersive region of the conductivity reveals the presence of a dielectric mechanism. The dc conductivity is an increasing function of the percentage w/w content in zeolite, as zeolite acts as an inherent source for protonation of the polymer. The dc component is suppressed by reducing the temperature from room temperature to liquid nitrogen temperature and the dielectric response may be determined as a function of temperature. The 25% w/w zeolite exhibits a frequency independent conductivity; i.e., it is free of dielectric loss. Low-frequency polarization phenomena are observed in 50% w/w zeolite accompanied by intense relaxation in the high-frequency limit. The frequencies f_{max} where a maximum of a loss peak is located vary with temperature by the Williams-Lander-Ferry law. The values of the activation energy of the relaxation process (which are of the order of polaronic dc conductivity) have the tendency to reach a minimum in the 25% w/w composition, which is a loss-free composite. The largest value is recorded in 50% w/w zeolite which suggests that ionic relaxation dominates in this composition. The temperature variation of the strength of the dielectric mechanism follows a Curie law, except for 50% w/w zeolite where the dielectric strength is practically constant. The relaxation frequency f_{max} and the dc conductivity (obtained from the dc plateau of the measured ac conductivity) follow qualitatively the same temperature law, but the parameters are quite different. It does not make sense to use the activation energy of the relaxation process which does not say anything about the conduction process. Additionally, f_{max} are significantly different than those predicted by the BNN model. It seems that the long-range electric charge transport (dc conductivity) and the relaxation that corresponds to short-range forward and backward localized motions involve different processes.

[1]K. Lee and A. J. Heeger, Phys. Rev. B **68**, 035201 (2003).
[2]V. N. Prigodin and A. J. Epstein, Synth. Met. **125**, 43 (2002).
[3]P. Malkaj, E. Vitoratos, and E. Dalas, (unpublished).
[4]M. Nakayama, J. Yano, K. Nakaoka, and K. Ogura, Synth. Met. **138**, 419 (2003).
[5]Weitkamp, M. Fritz, and S. Eritz, Int. J. Hydrogen Energy **20**, 967 (1995).
[6]C. Menardo, M. Nechtschein, A. Rousseau, and J. P. Travers, Synth. Met. **25**, 311 (1988).
[7]R. D. King, D. C. Nocera, and T. J. Pinnavaia, J. Electroanal. Chem. Interfacial Electrochem. **236**, 43 (1987).
[8]K. G. Fournaris, M. A. Karakasides, K. Yiannakopoulou, and D. Petridis, Chem. Mater. **11**, 2372 (1999).
[9]J. D. Dyre, J. Appl. Phys. **64**, 1456 (1988).
[10]S. R. Elliott, Adv. Phys. **36**, 135 (1987).
[11]N. F. Mott and E. Davis, *Electronic Processes in Non-crystalline Materials*, (Clarendon, Oxford, 1979), pp. 59–62.
[12]A. K. Jonscher, *Universal Relaxation Law*, (Chelsea Dielectrics, London, 1996), Chap. 5.
[13]H. Eyring, J. Chem. Phys. **4**, 283 (1936).
[14]M. L. Williams, R. F. Landel, and J. D. Ferry, J. Am. Chem. Soc. **77**, 3701 (1955).
[15]S. Sakkopoulos, E. Vitoratos, and E. Dalas, Synth. Met. **92**, 63 (1998).
[16]S. Capaccioli, M. Luccher, and G. Ruggeri, J. Phys.: Condens. Matter **19**, 5595 (1998).
[17]L. Barton, *La relaxation dielectrique de quelques verres ternaires oxyde acalin oxyde alcalino-terreux*, Verres et Refr. 20, 328 (1966).
[18]T. Nakajima, Conference on Electric Insulation and Dielectric Phenomena, National Academy of Sciences, Washington, DC, 1972.
[19]H. Namikawa, J. Non-Cryst. Solids **18**, 173 (1975).
[20]E. Singh, A. K. Narula, R. P. Tandon, A. Mansingh, and S. Chandra, J. Appl. Phys. **80**, 985 (1996).
[21]R. Singh and A. K. Narula, Synth. Met. **82**, 245 (1996).
[22]P. Sheng, B. Abeles, and Y. Arie, Phys. Rev. Lett. **31**, 44 (1973).